



Effect of viscoelastic postseismic relaxation on estimates of interseismic crustal strain accumulation at Yucca Mountain, Nevada

William C. Hammond,¹ Corné Kreemer,¹ Geoffrey Blewitt,¹ and Hans-Peter Plag¹

Received 3 February 2010; accepted 16 February 2010; published 27 March 2010.

[1] We estimate the long-term crustal strain rate at Yucca Mountain (YM), Nevada from GPS velocities taking into account viscoelastic relaxation following recent earthquakes to remove bias associated with transient deformation. The YM data reveal postseismic relaxation in time series non-linearity and geographic variation of the transient signal. From the data we estimate best-fitting lower crust and upper mantle viscosities of $10^{19.5}$ Pa s and $10^{18.5}$ Pa s, respectively. Once the relaxation model predictions are subtracted from the data, the long-term shear strain accumulation rate is between 16.3 and 25.1 nanostrains/year (ns/yr) to 99% confidence, a range much larger than the formal uncertainties from GPS measurement. We conclude that 1) a Maxwell viscoelastic model cannot explain all the deformation observed at YM, 2) uncertainty in viscosities dominates uncertainty in YM strain rates, and 3) the effects of large, recent earthquakes must be accounted for in seismic hazard studies using GPS. **Citation:** Hammond, W. C., C. Kreemer, G. Blewitt, and H.-P. Plag (2010), Effect of viscoelastic postseismic relaxation on estimates of interseismic crustal strain accumulation at Yucca Mountain, Nevada, *Geophys. Res. Lett.*, 37, L06307, doi:10.1029/2010GL042795.

1. Introduction

[2] Since 1999 a dense network of GPS stations has operated continuously to monitor the patterns and rates of strain in the crust near the proposed Yucca Mountain, Nevada high-level nuclear waste repository. This instrumentation makes important contributions to evaluating the suitability of the site since it measures the deformation of the crust, complementing geologic and seismic constraints on hazard. Recent analyses of the GPS data have determined that ~ 20 ns/yr (~ 1.2 mm/yr across ~ 60 km, Figure 1) of deformation occurs across the network [*Savage et al.*, 2001a]. This network lies east of, and adjacent to, the southern Walker Lane/eastern California Shear zone (SWL), which accommodates about $\sim 20\%$ of the relative motion between the Pacific and North America (NA) plates [*Dokka and Travis*, 1990]. The similarity of strain style and direction between the SWL and YM areas supports the hypothesis that it is tectonic in origin. However, more recent studies found that the strain rate is too large to be associated with SWL faults to the west, suggesting that it could be

related to structures local to YM [*Wernicke et al.*, 2004; *Hill and Blewitt*, 2006].

[3] During the time of GPS monitoring, the 1999 Hector Mine earthquake occurred approximately 250 kilometers to the south of YM (Figure 1). A number of studies characterized postseismic deformations that followed this and the 1992 Landers event [e.g., *Shen et al.*, 1994; *Deng et al.*, 1998; *Owen et al.*, 2002; *Hudnut et al.*, 2002; *Fialko*, 2004]. In particular *Freed et al.* [2007] showed that because non-linear signals can be observed at least as far from the epicenters as YM, viscoelastic relaxation in the mantle is required. Other candidate mechanisms such as poroelastic rebound and after-slip, while possibly active, cannot explain the signals at YM. As GPS time series have become longer (now >10 years in duration), the resolution of crustal deformation has improved, affording a new opportunity to evaluate the impact of far-reaching transients on strain accumulation rates at YM.

[4] Characterizing long-wavelength viscoelastic transient signals in the data is critical because they can bias estimates of strain accumulation, and could give the false impression that it is not focused on discrete fault systems. Our approach is to infer viscosities that best explain the GPS signals and earthquake source parameter data. We assume that the relaxation signal is superimposed on a background secular velocity field representing the long-term deformation pattern. In the real Earth, complete relaxation is never reached because it is asymptotic and the recurrence time of earthquakes may be less than the relaxation time of the material [*Savage and Prescott*, 1978]. However, by subtracting the predictions from a viscoelastic earthquake cycle model from the GPS data we can estimate the underlying time-invariant motion, and the present rate of strain accumulation. Strain rates so corrected can be compared to slip rates obtained in geologic investigations.

2. Data and Analysis

[5] We consider data from 60 GPS stations near YM and the earthquakes that continuously recorded data from 1999 until 2009 with a minimum of gaps and steps owing to equipment changes. These include the 16 sites around YM that are a part of the BARGEN network established shortly before the Hector Mine earthquake (Figure 1). We processed these data to obtain time series of daily coordinates with respect to fixed NA (see auxiliary material for details).²

[6] The transient signal in the YM GPS cluster can be seen in the rate changes over 9 years after the Hector Mine

¹Nevada Bureau of Mines and Geology, University of Nevada, Reno, Nevada, USA.

²Auxiliary materials are available in the HTML. doi:10.1029/2009GL042795.

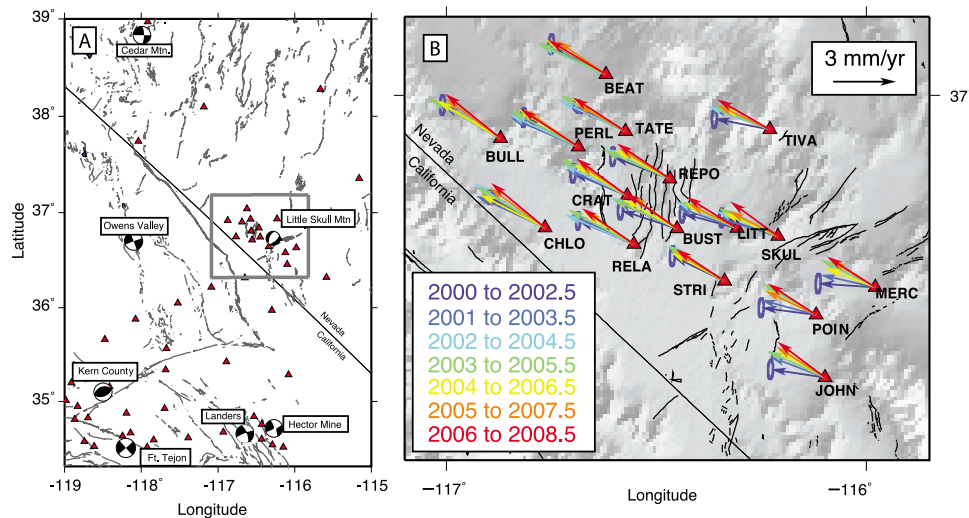


Figure 1. (a) Map of region showing mechanisms of earthquakes, GPS sites (red triangles) that were used in this analysis, and location of Yucca Mountain, Nevada (gray box). (b) GPS sites and rates with respect to NA as a function of time indicated by vector color (legend). Black lines are Quaternary faults. The 95% uncertainty ellipses are shown for the first time interval, and are similar for all time intervals.

event. We calculated rates for each 2.5-year time interval starting with an integral year for each site, with a model that includes amplitudes of annual and semiannual variations. Non-linear signals cause the rate azimuths to rotate to a more northerly direction over time because the rate change is greatest in the north component (Figure 1). Systematic rate changes are larger on the east side of YM (e.g., at sites JOHN, MERC, POIN, SKUL, TIVA) gradually decreasing to the west side, where the changes are not consistently greater than the uncertainties in the rates (Figure S1). For example, between 2000.0 and 2002.5 the site JOHN moved 0.4 mm/yr north and 2.6 mm/yr west, while from 2006 and 2008.5 the rate is 1.7 mm/yr north and 2.3 mm/yr west in our NA frame (Figure 2). Formal uncertainties of these rates for 2.5 year time series are 0.2 mm/yr, but may be larger when including time correlated noise. *Davis et al.* [2003] concluded that a realistic “whole error” uncertainty using data from the YM network was on average 0.15 mm/yr for time series 4.8 to 6.0 years in length, suggesting that uncertainty for our 2.5 year interval rates are likely larger. However, we computed the standard deviation of 2.5 year rates for the 21 northern Basin and Range GPS sites that were used to construct the reference frame (see auxiliary material for details) where the effects of relaxation were presumed to be negligible. These 2.5 year rates vary by between 0.1 and 0.5 mm/yr, with an average of 0.2 mm/yr, suggesting that this level of uncertainty is realistic, but could be as high as 0.5 mm/yr.

3. Modeling Postseismic Relaxation

[7] As input sources we use the seven largest and most recent earthquakes near YM (1857 Ft. Tejon M_W 8.2, 1872 Owens Valley M_W 7.6, 1932 Cedar Mountain M_S 7.2, 1952 Kern County M_L 7.2, 1992 Little Skull Mountain M_W 5.7, 1993 Landers M_W 7.3, and 1999 Hector Mine M_W 7.0, Figure 1 and Table S1). These events vary in style, size, and

location, and will contribute differently to the relaxation deformation field at YM. The smallest earthquake, Little Skull Mountain, was included because it was near the YM cluster, though its contribution is negligible in our final model.

[8] We use a Maxwell viscoelastic rheology to model the time dependence of stress relaxation of the lower crust and/or upper mantle. This rheology has been shown in many studies to adequately describe the time-dependent strains that follow large earthquakes [*Bürgmann and Dresen, 2008*]. Furthermore it is linear and hence allows us to sum the effects of multiple events occurring at different times in the past to estimate present day motions. We model the response of a spherically layered self-gravitating viscoelastic Earth following seismic dislocations using VISCOID v.3 [*Pollitz, 1997*] to predict the effect of the candidate earthquakes on the GPS time series. Inputs are the event parameters, the elastic shear, bulk moduli, and viscosities in intervals of depth (Figure S2). We assume a laterally homogeneous 15-km-thick purely elastic uppermost layer (upper crust) above a 15-km-thick viscoelastic lower crust with a Moho at 30-km depth, which is a simplification based on seismic constraints on crustal thickness [e.g., *Richards-Dinger and Shearer, 1997*] and depth of active seismicity [e.g., *Nazareth and Hauksson, 2004*]. The upper mantle extends from the bottom of the lower crust to a depth of 515 km. We vary the viscosities of the upper mantle and lower crust in a grid search with values from 10^{17} to 10^{21} Pa s, in logarithmic steps of one half order of magnitude. For each viscoelastic structure we calculate the total cumulative response between 1992.0 and 2010.0, spanning the time of GPS observation. We evaluate the cumulative response at densely sampled times after the Landers and Hector mine earthquakes (1, 3, 7, 15, 30, 100, 200 days) and yearly for other times, and use piece-wise cubic spline interpolation to estimate the cumulative postseismic displacement on each day $\Delta \mathbf{x}_{ps}(t, \eta_{LC}, \eta_{UM})$. We subtract the predictions of the

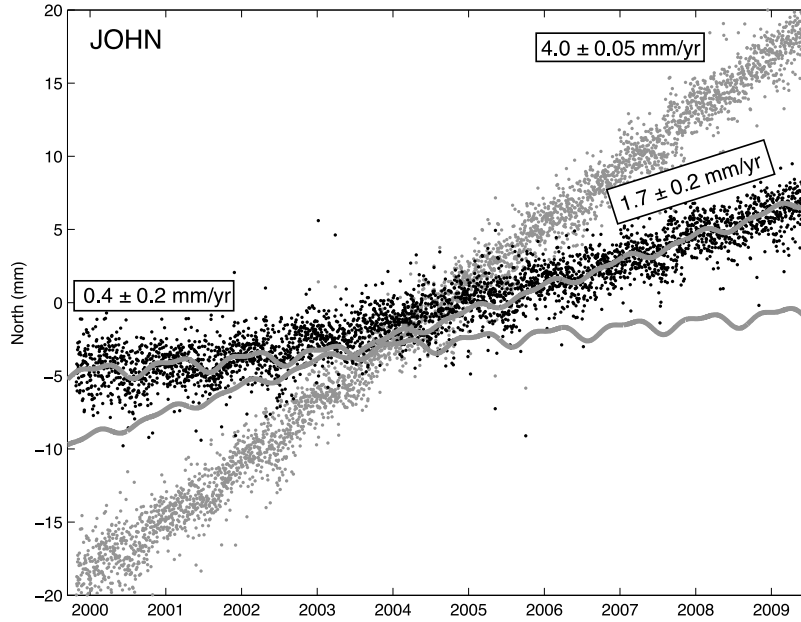


Figure 2. Black dots are north component time series for GPS site JOHN in a NA fixed reference frame for times after the Hector Mine earthquake. Wavy lines indicate the best fitting secular models for the first (2000.0 to 2002.5) and last (2006 to 2008.5) 2.5 years, with rate estimates. Gray dots indicate same but with correction for postseismic relaxation from all modeled earthquakes applied.

model from the GPS time series, and fit it with a function that includes the linear rate \mathbf{v} , intercept \mathbf{b} and seasonal terms

$$\mathbf{x}(t) - \Delta \mathbf{x}_{ps}(t, \eta_{LC}, \eta_{UM}) = \mathbf{b} + \mathbf{v}t + \sum_{i=1,2} [\mathbf{C}_i \cos(i\omega t) + \mathbf{S}_i \sin(i\omega t)] + \sum_{k=1}^M [\mathbf{D}_k H(t - t_k)] \quad (1)$$

where $\omega = 2\pi/\text{yr}$. Daily positions $\mathbf{x}(t)$ are $3 \times N$ vectors where N is the number of data in the time series. We include steps $H(t - t_k)$ to account for coseismic offsets (e.g., the Hector Mine earthquake) and equipment changes. The free parameters (\mathbf{b} , \mathbf{v} , \mathbf{C}_i , \mathbf{S}_i , and \mathbf{D}_k) are estimated using a least squares fit. The postseismic model time series have both non-zero slope and non-zero curvature, so correcting the time series will affect rates as well as remove transients to a degree that depends on the viscosities assumed (Figure 2).

4. Results

[9] Of the possible viscosity structures, which is the best model? If deviation from time series linearity is the result of postseismic relaxation, then time series curvature should be removed by subtracting the relaxation model from the data. We use a measure of linearity that compares the rate at the beginning and end of the corrected time series $\mathbf{x}(t) - \Delta \mathbf{x}_{ps}(t, \eta_{LC}, \eta_{UM})$

$$\chi_{dof}^2 = \frac{1}{dof} \sum_{i=1}^P \left[\frac{(v_{Ni1} - v_{NiM})^2}{\sigma_{Ni1}^2} + \frac{(v_{Ei1} - v_{EiM})^2}{\sigma_{Ei1}^2} \right] \quad (2)$$

where v_{Nij} , v_{Eij} represent the north and east velocities for site i (of P sites) for time interval j (of M intervals of 2.5 years). This measure of misfit does not require knowing the velocity before or a long time after the earthquakes since no particular rate before or after the correction is assumed.

Knowledge of the pre-event rate at YM sites would be useful, but is not available because the YM GPS sites were installed just a few months before the Hector Mine earthquake. We apply an F -test that depends on the number of degrees of freedom dof to identify models that are significantly worse than the best model. The non-linearity penalty excludes the model where no correction has been made. Using all the GPS sites, the lowest misfit occurs when $\eta_{LC} = 10^{19.5}$ Pa s and $\eta_{UM} = 10^{18.5}$ Pa s and excludes models with $\eta_{UM} > 10^{19}$ Pa s, $\eta_{UM} < 10^{18.5}$ Pa s and $\eta_{LC} < 10^{19}$ Pa s (Figure 3). Considering far-field sites alone (sites >100 km from Hector Mine) only excludes models with $\eta_{UM} < 10^{18.5}$ Pa s.

[10] For each viscoelastic structure we use the corrected time series to estimate the rate of crustal strain and rigid rotation parameters simultaneously [Savage *et al.*, 2001b]. These provide estimates of the long-term shear strain accumulation rate (Figure 3). Compared to the uncorrected shear strain rate (19.5 ± 0.8 ns/yr) some models reduce the shear strain rate while others increase it. If we only consider models that are not excluded by the linearity constraint to 95% confidence, we find that the shear strain rate is between 20.7 and 25.1 ns/yr. If we demand 99% confidence that the model is significantly worse, the interval widens to 16.3 to 25.1 ns/yr, and thus it is not certain whether the correction will increase or decrease the estimate of strain accumulation rate around YM. This interval is much larger than the formal uncertainties of the uncorrected strain rate, and thus uncertainty in viscoelastic structure dominates the uncertainty budget of long-term strain rate of the crust.

5. Discussion

[11] Repeating our analysis including only the postseismic model time series from the Landers and Hector Mine events shows that they provide the signal used to restrict the vis-

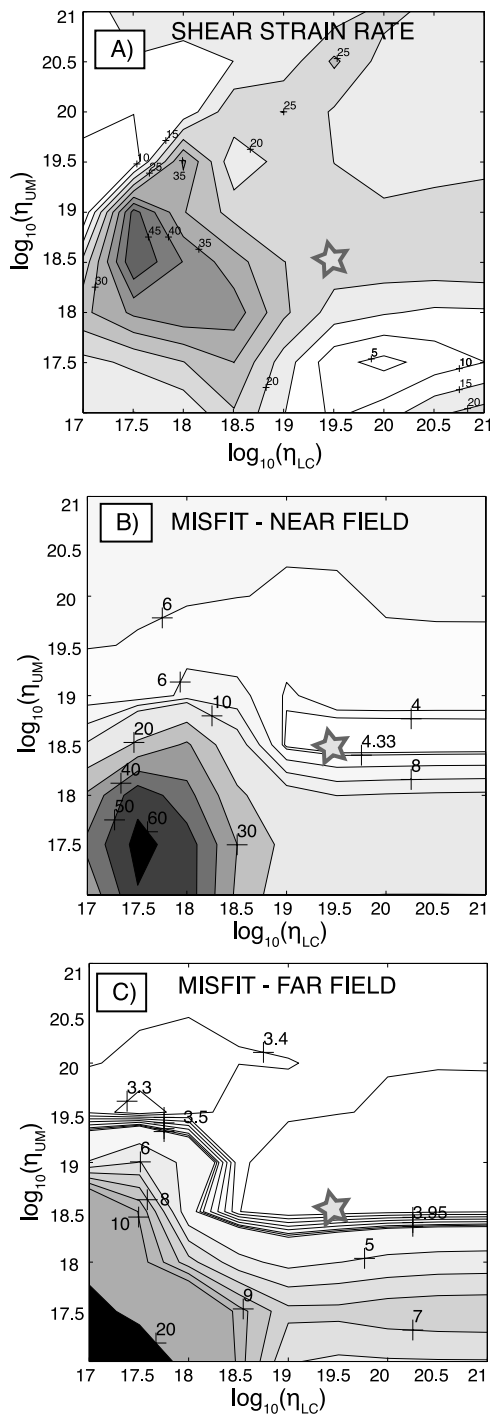


Figure 3. (a) Contours of shear strain rate estimated from GPS time series after correction for viscoelastic relaxation given indicated viscosity of the lower crust and upper mantle. (b) Contour of misfit as a function of viscosity in lower crust and upper mantle for near field sites only. (c) Same for far field sites only. Star in each plot indicates best fitting model with $\eta_{LC} = 10^{19.5}$ Pa s, $\eta_{UM} = 10^{18.5}$ Pa s.

coelastic structure, though there is a contribution to the velocity field from the older events. The older events cause contemporary deformation in the GPS velocity field around southern California and Nevada (Figure S3). They do not help to constrain the viscosities by causing time series

curvature because the changes in rates are too slow to be observed between 1999 and 2009. However, these events must be taken into account when estimating the long-term velocities from GPS data, e.g., when using them to evaluate slip rates on faults across southern California and Nevada. Velocities corrected for all the events we consider are shown in Figure S4.

[12] Owing to the long wavelength character of deformation (>200 km) attributable to viscoelastic relaxation of the upper mantle it is perhaps surprising that a geodetic rate change signal could vary over the relatively small aperture of the YM cluster. However, the geographic variation in changes in rate over time (Figure S1) can be explained by the location of the YM cluster just east of the north-northwest nodal plane associated with Hector Mine and Landers. This is where the models predict that lateral gradients in the postseismic signals are large (Figures S3b and S3c). Thus the YM GPS cluster is fortuitously located to detect postseismic relaxation from the Mojave earthquakes (Figure 1). This close match between model and data suggests that the viscoelastic process is of dominant importance in the far field and that YM rate changes are not attributable to other processes.

[13] While a rigorous comparison between geologic and geodetic data requires detailed analysis, an order of magnitude comparison may be informative. There are <10 sub-parallel normal fault systems across YM that exhibit Quaternary offset, and each accommodate in the range of 0.001 to 0.05 mm/yr (e.g., see *Whitney and Keefer* [2000] and chapters therein). So there has been at most ~ 0.01 to 0.5 mm/yr of strain release across YM in the recent geologic past. The upper end of this range may be an overestimate, but is similar to 0.6 mm/yr obtained when ~ 20 ns/yr GPS strain rate is expressed across the fault zone (~ 30 km). Thus the geologic rate is generally lower than the geodetic rate, and thus we might expect the viscoelastic correction to reduce the inferred long-term strain rate to bring these into agreement. Using integrated GPS and geologic constraints imply a strain rate on the lower end of our estimated range (~ 16 ns/yr), and that the higher end of the geologic rates are more likely.

[14] GPS data and rock mechanics experiments suggest that more complex or non-linear rheology, rather than the Maxwell model we have assumed, control mantle deformation and cause a stronger time series curvature in the weeks to months following an earthquake [e.g., *Karato and Wu*, 1993; *Bürgmann and Dresen*, 2008]. However, the time series curvature we observe at the YM sites following the Hector Mine event is well-explained by our model, and do not exhibit a rapid early-stage relaxation (Figure 2), in contrast to sites closer to the Hector Mine epicenter [*Pollitz et al.*, 2001]. Whether this is because these signals are too small to be observed at far field sites, or whether the far-field and near-field responses are qualitatively different, is uncertain. If non-linear effects are important, then better modeling of the near-field data (e.g., by including the possible contributions from afterslip and poroelastic rebound) will be required to separate the contributions of non-linear effects. Neither have we considered the effects of lateral heterogeneity in elastic and viscous properties [e.g., *Malservisi et al.*, 2001]. Such variations are present since seismic velocities [e.g., *Goes and van der Lee*, 2002] and depth to Moho [e.g., *Gilbert and Sheehan*, 2004] vary

substantially across southern California. Adding a greater number of layers, more complex rheology and/or lateral heterogeneity in elastic and viscous properties will improve the fit to the GPS data, particularly in the near-field. Including other sources of epistemic uncertainty in rheology and structure will tend to increase the uncertainty in long-term strain rate, and thus the uncertainties we provide are a minimum. However, our simple model explains the magnitude and geographic variation of the geodetic transient signals at YM, and implies a viscosity structure similar to those found in most previous studies of the Basin and Range (e.g., the majority of which find $\eta_{LC} > \eta_{UM}$ and η_{UM} between 10^{18} to 10^{19} Pa s (see summary table of Hammond et al. [2009])). Thus this type of modeling offers the promise that postseismic transients can be identified and separated from secular deformation over large geographic areas, and that the impact that these adjustments have on GPS estimates of seismic hazard can be evaluated.

[15] **Acknowledgments.** This research was supported by DOE Yucca Mountain Project/NSHE Cooperative Agreement DE-FC28-04RW12232, task ORD-FY04-003. We wish to thank Jim Davis for early discussions and sharing of his results. GPS data archiving was provided by UNAVCO, Inc. Additional support to WCH, CK and GB was provided by NSF EAR projects 0610031 and 0635757. We are grateful to the International GNSS Service for providing GPS data, and to the Jet Propulsion Laboratory for software and GPS products. F. Pollitz and W. Thatcher provided comments that improved this manuscript.

References

- Bürgmann, R., and G. Dresen (2008), Rheology of the lower crust and upper mantle: Evidence from rock mechanics, geodesy, and field observations, *Annu. Rev. Earth Planet. Sci.*, *36*, 531–567, doi:10.1146/annurev.earth.36.031207.124326.
- Davis, J. L., R. A. Bennett, and B. P. Wernicke (2003), Assessment of GPS velocity accuracy for the Basin and Range Geodetic Network (BARGEN), *Geophys. Res. Lett.*, *30*(7), 1411, doi:10.1029/2003GL016961.
- Deng, J., M. Gurnis, H. Kanamori, and E. Hauksson (1998), Viscoelastic flow in the lower crust after the 1992 Landers, California, earthquake, *Science*, *282*, 1689–1692, doi:10.1126/science.282.5394.1689.
- Dokka, R. K., and C. J. Travis (1990), Role of the Eastern California Shear Zone in accommodating Pacific-North-American plate motion, *Geophys. Res. Lett.*, *17*, 1323–1326, doi:10.1029/GL017i009p01323.
- Fialko, Y. (2004), Evidence of fluid-filled upper crust from observations of postseismic deformation due to the 1992 M_w 7.3 Landers earthquake, *J. Geophys. Res.*, *109*, B08401, doi:10.1029/2004JB002985.
- Freed, A. M., R. Bürgmann, and T. A. Herring (2007), Far-reaching transient motions after Mojave earthquakes require broad mantle flow beneath a strong crust, *Geophys. Res. Lett.*, *34*, L19302, doi:10.1029/2007GL030959.
- Gilbert, H., and A. F. Sheehan (2004), Images of crustal variations in the intermountain west, *J. Geophys. Res.*, *109*, B03306, doi:10.1029/2003JB002730.
- Goes, S., and S. van der Lee (2002), Thermal structure of the North American uppermost mantle inferred from seismic tomography, *J. Geophys. Res.*, *107*(B3), 2050, doi:10.1029/2000JB000049.
- Hammond, W. C., C. Kreemer, and G. Blewitt (2009), Geodetic constraints on contemporary deformation in the northern Walker Lane: 3. Postseismic relaxation in the central Nevada seismic belt, in *Late Cenozoic Structure and Evolution of the Great Basin–Sierra Nevada Transition*, edited by J. S. Oldow and P. Cashman, *Spec. Pap. Geol. Soc. Am.*, *447*, 33–54.
- Hill, E. M., and G. Blewitt (2006), Testing for fault activity at Yucca Mountain, Nevada, using independent GPS results from the BARGEN network, *Geophys. Res. Lett.*, *33*, L14302, doi:10.1029/2006GL026140.
- Hudnut, K. W., et al. (2002), Continuous GPS observations of postseismic deformation following the 16 October 1999 Hector Mine, California, earthquake (M_w 7.1), *Bull. Seismol. Soc. Am.*, *92*, 1403–1422, doi:10.1785/0120000912.
- Karato, S., and P. Wu (1993), Rheology of the upper mantle: A synthesis, *Science*, *260*, 771–778, doi:10.1126/science.260.5109.771.
- Malservisi, R., K. P. Furlong, and T. H. Dixon (2001), Influence of the earthquake cycle and lithospheric rheology on the dynamics of the Eastern California Shear Zone, *Geophys. Res. Lett.*, *28*, 2731–2734, doi:10.1029/2001GL013311.
- Nazareth, J. J., and E. Hauksson (2004), The seismogenic thickness of the southern California crust, *Bull. Seismol. Soc. Am.*, *94*, 940–960, doi:10.1785/0120020129.
- Owen, S., et al. (2002), Early postseismic deformation from the 16 October 1999 M_w 7.1 Hector Mine, California, earthquake as measured by survey-mode GPS, *Bull. Seismol. Soc. Am.*, *92*, 1423–1432, doi:10.1785/0120000930.
- Pollitz, F. F. (1997), Gravitational-viscoelastic postseismic relaxation on a layered spherical Earth, *J. Geophys. Res.*, *102*, 17,921–17,941, doi:10.1029/97JB01277.
- Pollitz, F. F., C. W. Wicks, and W. Thatcher (2001), Mantle flow beneath a continental strike slip fault: Postseismic deformation after the 1999 Hector Mine earthquake, *Science*, *293*, 1814–1818, doi:10.1126/science.1061361.
- Richards-Dinger, K. B., and P. M. Shearer (1997), Estimating crustal thickness in southern California by stacking PmP arrivals, *J. Geophys. Res.*, *102*, 15,211–15,224, doi:10.1029/97JB00883.
- Savage, J. C., and W. H. Prescott (1978), Asthenosphere readjustment and the earthquake cycle, *J. Geophys. Res.*, *83*, 3369–3376, doi:10.1029/JB083iB07p03369.
- Savage, J. C., W. Gan, and J. L. Svarc (2001a), Strain accumulation and rotation in the Eastern California Shear Zone, *J. Geophys. Res.*, *106*, 21,995–22,007, doi:10.1029/2000JB000127.
- Savage, J. C., J. L. Svarc, and W. H. Prescott (2001b), Strain accumulation near Yucca Mountain, Nevada, 1993–1998, *J. Geophys. Res.*, *106*, 16,483–16,488, doi:10.1029/2001JB000156.
- Shen, Z. K., et al. (1994), Postseismic deformation following the Landers earthquake, California, 28 June 1992, *Bull. Seismol. Soc. Am.*, *84*, 780–791.
- Wernicke, B., J. L. Davis, R. A. Bennett, J. E. Normandeau, A. M. Friedrich, and N. A. Niemi (2004), Tectonic implications of a dense continuous GPS velocity field at Yucca Mountain, Nevada, *J. Geophys. Res.*, *109*, B12404, doi:10.1029/2003JB002832.
- Whitney, J. W., and W. R. Keefer (2000), Geologic and geophysical characterization studies of Yucca Mountain, Nevada, a potential high-level radioactive-waste repository, *U.S. Geol. Surv. Digital Data Ser.*, *58*.

G. Blewitt, W. C. Hammond, C. Kreemer, and H.-P. Plag, Nevada Bureau of Mines and Geology, University of Nevada, MS 178, Reno, NV 89557-0088, USA. (whammond@unr.edu)